Regularization using truncated singular value decomposition for estimating the Fourier spectrum of a noised space distribution over an extended support

Waseem Al Hadad, Denis Maillet, Stéphane André, Benjamin Rémy

LEMTA, University of Lorraine and CNRS
ENSEM – 2 avenue de la Forêt de Haye – TSA60604
54518 Vandœuvre-lès-Nancy cedex, France
e-mail: denis.maillet@univ-lorraine.fr

This paper is devoted to a theoretical and numerical study of different ways of calculating the Fourier transform of a noisy signal where the boundary conditions at the lateral boundaries of the measurement interval are not precisely known. This happens in different characterization problems where infrared camera is used for temperature measurements. In order to overcome this difficulty, the interval where the Fourier transform (its support) is supposed to be larger than the measurement domain is defined. Thus, this virtual interval larger than the measurement interval is used. We show that regularization by truncated singular value decomposition is able to yield good estimates to this very ill-posed inverse problem.

Keywords: integral transforms, thermal quadrupoles, heat transfer in mini-channel, inverse heat conduction and convection.

1. Introduction

We consider here the problem of reconstructing the Fourier spectrum of N_x noisy discrete temperature measurements θ_i made on a solid surface, which is for discrete abscissa $x_i \in\ ]-\ell;\ \ell] \subset\ ]-L;\ L]$ for $i = 1$ to N_x, in a 2D heat transfer case. The $N_h = 2n_h$ harmonics of this spectrum are

$$\widetilde{\theta}_n = \int_{-L}^{L} \theta(x) \exp(-\mathrm{i}\alpha_n x)\mathrm{d}x \quad \text{with} \quad \mathrm{i}^2 = -1, \quad L \geq \ell,$$

(1)

$$\text{and} \quad \alpha_n = n\pi/L \quad (\text{for} \quad n = -n_h + 1,\ -n_h + 2, \cdots, -1,\ 0,\ 1,\ 2, \cdots, n_h - 1,\ n_h).$$

Estimation of this spectrum is required in thermal characterization experiments where infrared thermography (IR) is used. We take as example thermal diffusivity measurement of a composite flat plate made of anisotropic material with a front face flash excitation and rear face IR temperature measurement [1] or for estimating the heat fluxes at different interfaces of a mini-channel heated locally over its front face (either steady state or transient heating), using front or rear face IR temperature measurement [2–4]. This stems from the fact that an analytical solution of this type of heat transfer problem can be obtained very easily using the Fourier integral transform over a finite space domain, for example, through the thermal quadrupoles technique [5]. Inversion of the corresponding experimental temperature distribution, written in the Fourier domain, can be applied either to estimate thermophysical parameters of a sample (a parameter estimation problem) [1] or to recover temperature and fluxes at different interfaces as well as the bulk temperature distribution in a conjugated (fluid flow/wall) heat transfer (inverse function estimation problem based on inverse heat conduction/convection) [2–4].

The main difficulty in this type of configuration is that the experimental boundary conditions at $x = \pm\ell$ are generally not precisely known: heat flux in the x direction by both natural convection and radiation can occur in the anisotropic diffusivity characterization problem [1] or the channel wall length $2L$ can be larger than the measurement length 2ℓ in the channel thermal characterization problem [2], which means that neither temperature nor heat flux are equal to zero at the two boundaries, especially at the downstream one if it is too close to the heated region (at $x = \ell$ if the fluid flows in the positive x direction).

If the eigenvalues $\alpha'_n = n\pi/\ell$ are chosen, which correspond to the zero temperature or flux boundary conditions, the solution of the direct or the inverse problem may be biased.

This is why the authors decided to define the eigenvalues $\alpha_n = n\pi/L$ over a larger interval $]-L; L]$, called here a 'virtual' interval, wider than the measurement interval $]-\ell; \ell]$, see Eq. (1), where $k_v = L/\ell \geq 1$. If k_v becomes large enough, the virtual boundaries $x = \pm L$ are far enough from the heat source, which lays inside the $]-\ell; \ell]$ measurement interval and the zero temperature or flux boundary conditions become valid, and the α_n eigenvalues become exact.

2. THE STUDIED FUNCTION

We consider here the following function (2) which is plotted in Fig. 1:

$$\begin{aligned}
\theta(x) &= 0 && \text{for} \quad x \in]-L_0; \ 0], \\
\theta(x) &= Ax^2 \exp\left(-B\frac{x}{L_0}\right) && \text{for} \quad x \in]0; \ L_0],
\end{aligned} \qquad (2)$$

where A and B are the parameters of this function (here $A = 1.2 \times 10^5$ °C.m^{-2} and $B = 14.4$ with $L_0 = 80$ mm. The exact analytical spectrum of this function is

$$\widetilde{\theta}_n^{exact} = \frac{A}{K^2}\left[-KL_0^2 \exp(-KL_0) - 2L_0 \exp(-KL_0) - \frac{2}{K}\left\{\exp(-KL_0) - 1\right\}\right], \qquad (3)$$

where

$$K = \frac{B}{L_0} + i\alpha_n.$$
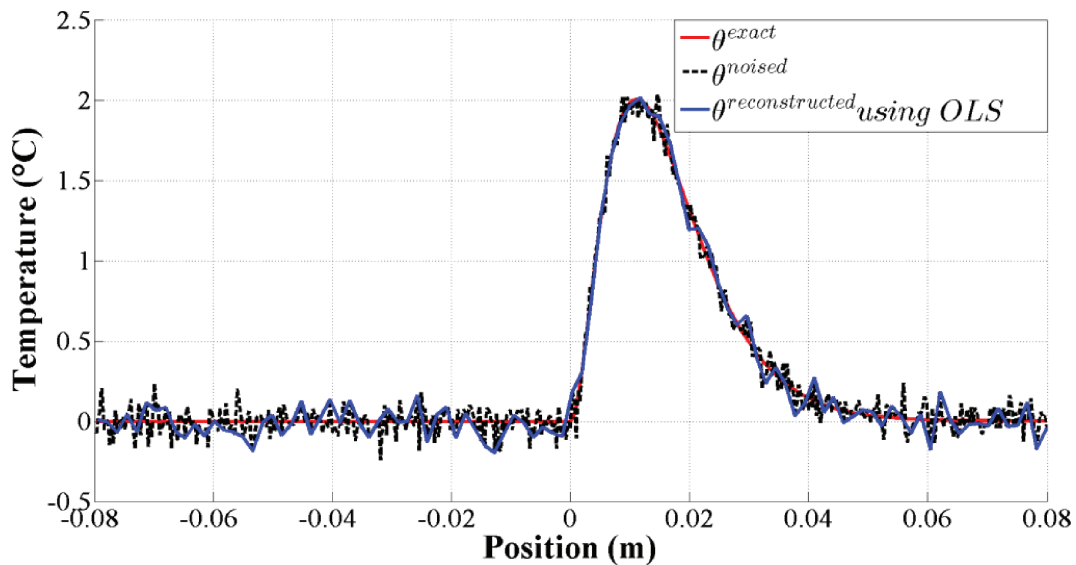
Fig. 1. Exact (Eq. (2)), noised (Eq. (4)) and reconstructed (Eq. (9)) temperature profiles for $N_x^{2L_0} = 492$ points.

An identically independently distributed noise ε_i of standard deviation $\sigma = 0.08°C$ is added at each location (see Fig. 1) $x_i = -L_0 + i\Delta x$, for $i = 1$, to $N_x^{2L_0} = 492$, where $\Delta x = 2L_0/N_x^{2L_0}$:

$$\theta_i^{noised} = \theta(x_i) + \varepsilon_i. \tag{4}_1$$

This generates a synthetic temperature measurement vector of size $N_x^{2L_0} \times 1$:

$$\boldsymbol{\theta}^{noised} = \boldsymbol{\theta} + \boldsymbol{\varepsilon}, \qquad \text{where} \qquad \text{E}(\boldsymbol{\varepsilon}) = \boldsymbol{0} \qquad \text{and} \qquad \text{cov}(\boldsymbol{\varepsilon}) = \sigma^2 \boldsymbol{I}_{N_x^{2L_0}}, \tag{4}_2$$

where E () is the expectancy of a random column vector, cov() its variance-covariance matrix and $\boldsymbol{I}_{Nx}$ the identity matrix of size $N_x^{2L_0}$.

2.1. Noisy data available on the whole interval of length $2L_0$

Since the zero temperature and flux boundary conditions are valid at $x = \pm L_0$ (see Fig. 1), the α_n eigenvalues $\alpha_n = n\pi/L_0$ become exact. For this reason we will use here $k_v = 1$. The N_h harmonics of the temperature profile (3) can be generated in a $\widetilde{\boldsymbol{\theta}}^{exact}$ column vector of size N_hx1 (see its energy spectrum in Fig. 2). Once the synthetic (pseudo-experimental) temperature profile $\boldsymbol{\theta}^{noised}$ is known, the unknown spectrum $\widetilde{\boldsymbol{\theta}}$ can be calculated in two different ways:

a) Spectrum assessment by direct numerical quadrature

This technique is the simplest one, it consists in calculating an approximation of the definition (1) of each harmonic $\widetilde{\theta}_n$ through a numerical integration of the noised signal [6]:

$$\widetilde{\theta}_n \approx \Delta x \sum_{i=1}^{N_x^{2L_0}} \theta_i^{noised} \exp(-i\alpha_n x_i) = \sum_{i=1}^{N_x^{2L_0}} G_{ni}\theta_i^{noised} \quad \text{with} \quad G_{ni} = \exp(-i\alpha_n x_i)\Delta x. \tag{5}$$

Since $N_x^{2L_0}$ data θ_i^{noised} are available, a number $N_h = 2n_h \leq N_x^{2L_0}$ of harmonics can be calculated. This technique can provide good approximations of the harmonics of low order (low values of $|n|$) but its precision decreases for high space frequencies, because of the presence of noise in the signal. In this paper this technique is not used, we will use only technique (b).

b) Spectrum estimation by inverse discrete Fourier transform

Instead of using the approximation of an integral of a noised signal (5), it is better to consider estimation of its spectrum as an inverse problem. So, we can start with an exact model, which is the definition of the inverse Fourier transform for an exact output signal $\boldsymbol{\theta}$ depending on a limited number of harmonics $N_h = 2n_h = N_x^{2L_0}$:

$$\theta(x_i) = \theta_i = \frac{1}{2L_0} \sum_{n=-n_h+1}^{n_h} \widetilde{\theta}_n \exp(+i\alpha_n x_i) = \sum_{n=-n_h+1}^{n_h} S_{in}\widetilde{\theta}_n \tag{6}$$

$$\text{with} \qquad S_{in} = \frac{1}{2L_0} \exp(+i\alpha_n x_i).$$

This equation can be expressed in a matrix/column vector form, if the subscripts of the $\widetilde{\theta}_n$ harmonics are increased by a simple translation equal to n_h, in order not to have any negative index in the components of the spectrum vector $\widetilde{\boldsymbol{\theta}}$, that is $[\widetilde{\boldsymbol{\theta}}]_k = \widetilde{\theta}_{k-n_h}$. This spectrum vector, a parameter vector to be estimated as well as the corresponding model is

$$\widetilde{\boldsymbol{\theta}} = [\; \widetilde{\theta}_{-n_h+1} \quad \widetilde{\theta}_{-n_h+2} \quad \cdots \quad \widetilde{\theta}_0 \quad \cdots \quad \widetilde{\theta}_{n_h-1} \quad \widetilde{\theta}_{n_h} \;]^T \qquad \text{and} \qquad \boldsymbol{\theta} = \boldsymbol{S}\widetilde{\boldsymbol{\theta}}, \tag{7}$$

where the coefficients of the matrix $\boldsymbol{S}$ of size $N_x^{2L_0}$ are $[\boldsymbol{S}]_{ik} = S_{i,k-n_h}$. So, the ordinary least square (OLS) solution for $N_h = N_x^{2L_0}$ and for a square matrix $\boldsymbol{S}$ is

$$\widehat{\widetilde{\boldsymbol{\theta}}}_{OLS}^{square} = \arg(\min(J(\widetilde{\boldsymbol{\theta}}))) = \boldsymbol{S}^{-1}\boldsymbol{\theta}^{noised}$$

$$\text{where} \qquad J(\widetilde{\boldsymbol{\theta}}) = \left\|\boldsymbol{r}(\widetilde{\boldsymbol{\theta}})\right\|^2 \qquad \text{with} \qquad \boldsymbol{r}(\widetilde{\boldsymbol{\theta}}) = \boldsymbol{\theta}^{noised} - \boldsymbol{S}\widetilde{\boldsymbol{\theta}}. \tag{8}$$

Here, the inverse problem is very well posed, since the condition number of matrix $\boldsymbol{S}$ is very close to unity, which means that the residual vector $\boldsymbol{r}(\widehat{\widetilde{\boldsymbol{\theta}}}_{OLS}^{square})$ is very small. The recalculated (reconstructed) signal can be written as

$$\theta^{recalc} = \boldsymbol{S}\widehat{\widetilde{\boldsymbol{\theta}}}_{OLS}^{square}. \tag{9}$$

The reconstructed signal is plotted together with the exact signal $\boldsymbol{\theta}$ and with the noised signal $\boldsymbol{\theta}^{noised}$ in Fig. 1. One can see that the fit is perfect.

The spectral energy density $\widetilde{\boldsymbol{\theta}}_n^*\widetilde{\boldsymbol{\theta}}_n$ (the upper star designates the transpose of the complex conjugate) of the exact temperature profile, as well as its estimated value that stems from the ordinary least square estimation (8) deduced from the noised temperature profile, is plotted in Fig. 2. Since the analytical and estimated spectra outside the $]-40;\ 40]$ interval are equal to zero, we show here only the spectra for this interval. We can see that all the harmonics are very well estimated except the $n = 0$ harmonic (peak) that is lower than its true value. The noise in the discrete simulated measurements is the only cause of this error.
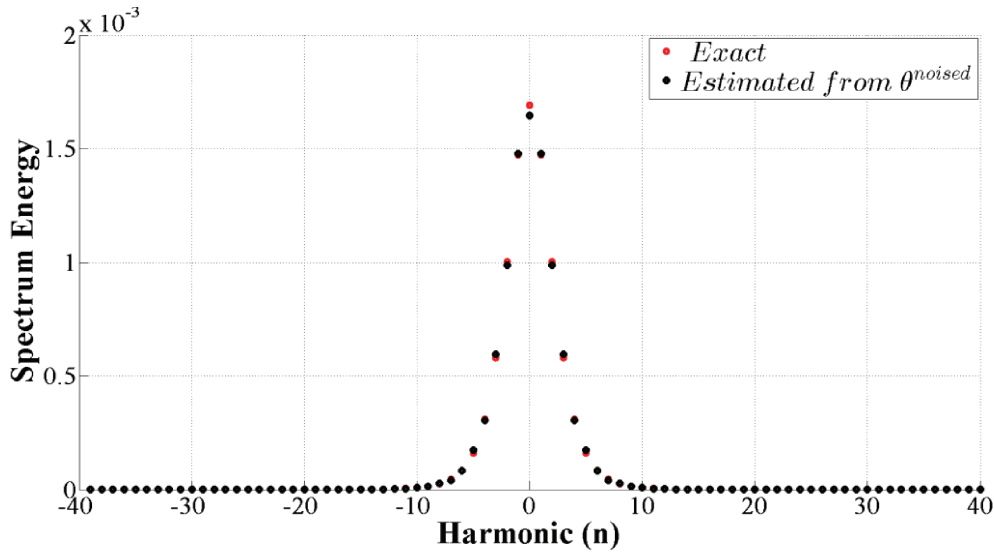
Fig. 2. Spectral energy densities of temperature profile: exact $(\widetilde{\boldsymbol{\theta}}_n^*\widetilde{\boldsymbol{\theta}}_n)$ and estimated $(\widehat{\widetilde{\boldsymbol{\theta}}}_{OLS}^{*square}\widehat{\widetilde{\boldsymbol{\theta}}}_{OLS}^{square})$.

2.2. Noisy data available over a part of the $2L_0$ interval

Now let us consider the case where we only know a part of the profile (here, we suppose that we only know $N_x = 200$ points over $]-\ell;\ \ell]$, where $N_x < N_x^{2L_0}$, see Fig. 3). Our aim here is to estimate the spectrum of this profile, which has to be as close as possible to the "true" spectrum shown in Fig. 2 corresponding to the $]-L_0;\ L_0]$ interval. We suppose here that L_0 corresponding to homogeneous boundary conditions is unknown and that $\ell = 32.5$ mm remains fixed and $L \leq L_0 = 80$ mm will be changed. In the following sub-sections, we will show the spectrum estimation of this profile for two

cases: the first case $k_{\mathrm{v}} = 1(L = \ell)$, in which the eigenvalues are set on the small interval $\alpha'_n = n\pi/\ell$ and the second case $k_{\mathrm{v}} = 2(L = 2\ell)$, in which the eigenvalues are calculated on the larger interval $\alpha_n = n\pi/2\ell$.
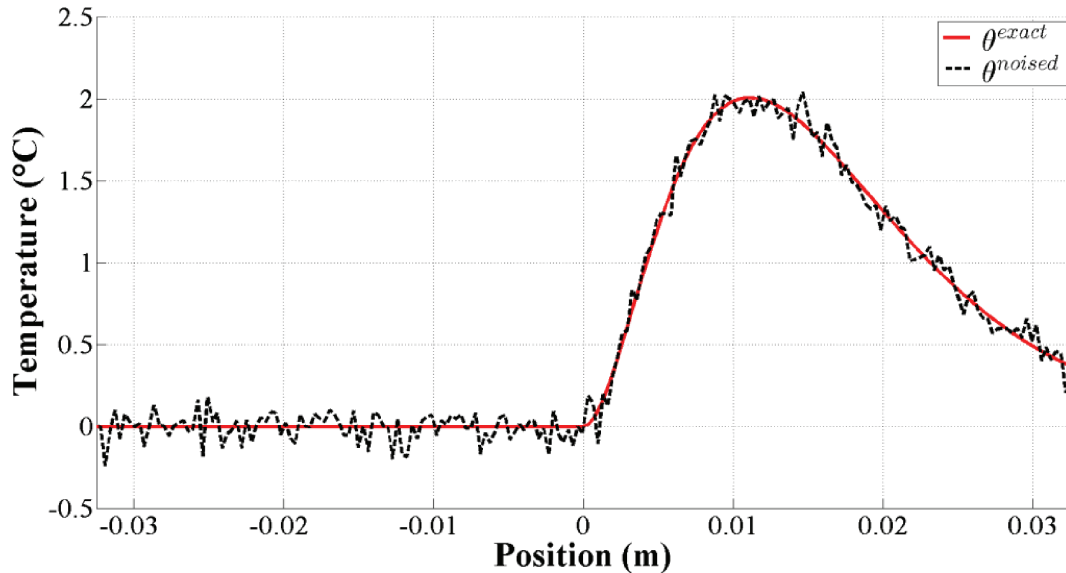
Fig. 3. Exact and noised temperature profiles over $]-\ell;\ \ell]$ with $\ell = 0.0325$ m and $N_x = 200$.

2.2.1. Estimation of the Fourier spectrum without any virtual length $(k_{\mathrm{v}} = 1)$

In this case no regularization is needed since condition number of **S** is equal to 1 (see Fig. 6 further in this paper). Figure 4 shows a very good agreement between the noisy profile and the profile recalculated from an estimated spectrum. But the use of the eigenvalues that do not satisfy the boundary conditions leads to a biased estimation of the defined exact spectrum, for reference, over the $2L_0$ length (see Fig. 5).
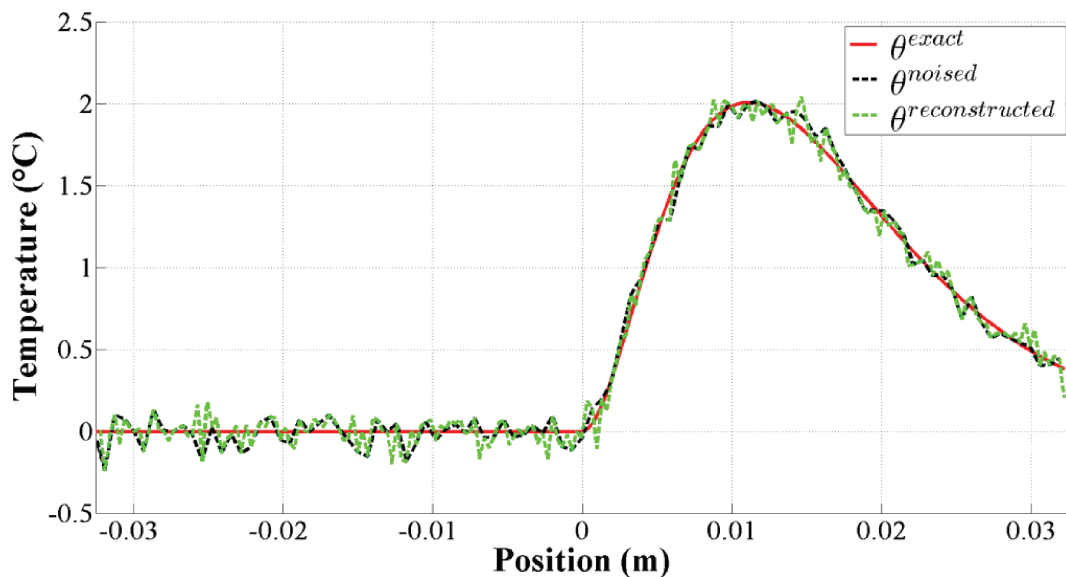
Fig. 4. Exact, noised and reconstructed temperature profiles over $]-\ell;\ \ell]$ using ordinary least squares $N_x = 200$ points $(k_{\mathrm{v}} = 1)$.
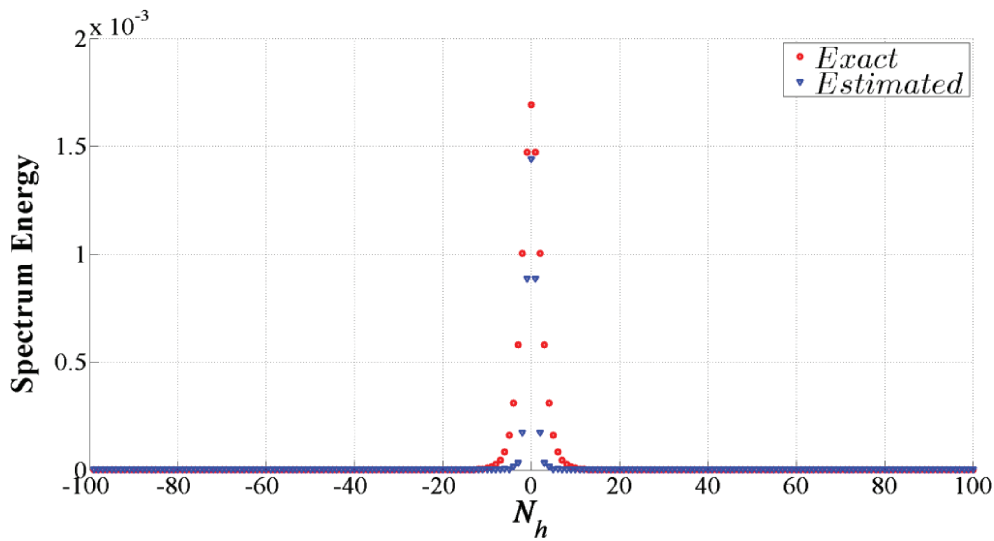
Fig. 5. Estimated spectrum of noisy profile over $]-\ell; \ell]$ without regularization ($k_{\mathrm{v}} = 1$).

2.2.2. Estimation of the Fourier spectrum with a virtual length ($k_{\mathrm{v}} = 2$)

Here, we show how the spectrum of the noisy profile can be estimated using the measurement over a part of its support. The N_x noised temperatures are known on the $]-\ell; \ell]$ interval, and the integral Fourier transform (1) is defined on the $]-L; L]$ interval with $L = 2\ell$ and, as a consequence, the N_x new eigenvalues $\alpha_n = \dfrac{n\pi}{L} = \dfrac{n\pi}{2\ell}$ are used. They are the halves of the preceding ones (case $L = \ell$). This means that the distribution of the space frequencies used for parameterizing the $\theta(x)$ profile is more dense than in the case $k_{\mathrm{v}} = 1$.

If we calculate square matrix $\boldsymbol{S}$ using eigenvalues defined on the $]-L; L]$ interval and the information points (here N_x points) chosen on interval $]-\ell; \ell]$ it becomes very ill-conditioned. Consequently, very poor estimates of the spectrum are obtained: for a linear system the relative error of the estimated spectrum can be expressed as the product of the condition number of the matrix $\boldsymbol{S}$ and the relative error of the measurement. We know in reality it is impossible to make a measurement without noise. So in the presence of the noise it is impossible to estimate the spectrum if matrix $\boldsymbol{S}$ is ill-conditioned. Normally to overcome this difficulty, we use a regularization to make the inverse problem well-conditioned. In the following subsections (I and II), we present two regularization techniques that have been applied to the synthetic profile. In another work, the same technique has been applied to experimental IR temperature measurements for a flat mini-channel in a transient heating case [4].

I. Rectangular estimation

We know that the maximum number of harmonics that can be estimated cannot exceed the number of space points ($N_h = 2n_h \leq N_x$). If there is no abrupt change in the experimental profile, there is no need for many harmonics to reconstruct this profile. So we can estimate a number of harmonics α to be lower than the number of measurements N_x. In this case, matrix $\boldsymbol{S}$ can be replaced by a rectangular matrix $\boldsymbol{S}_\alpha$ with the size $N_x \mathrm{x} \alpha$ (the $(N_x - \alpha)/2$ first column as well as the $(N_x - \alpha)/2$ last columns of $\boldsymbol{S}$ have been removed) and the ordinary least square solution becomes

$$\widehat{\widetilde{\boldsymbol{\theta}}}_{OLS,\alpha}^{\,rect} = \arg(\min(J(\widetilde{\theta}_\alpha))) = (\boldsymbol{S}_\alpha^* \boldsymbol{S}_\alpha)^{-1} \boldsymbol{S}_\alpha^* \boldsymbol{\theta}^{\,noised},$$

$$\text{where} \qquad J(\widetilde{\boldsymbol{\theta}}_\alpha) = \left\| \boldsymbol{r}(\widetilde{\boldsymbol{\theta}}_\alpha) \right\|^2 \qquad \text{with} \qquad \boldsymbol{r}(\widetilde{\boldsymbol{\theta}}) = \boldsymbol{\theta}^{\,noised} - \boldsymbol{S}_\alpha \widetilde{\boldsymbol{\theta}}_\alpha. \tag{10}$$

The matrix S_α^* is the adjoint of complex matrix S_α, which is the transpose of its conjugate $(S_\alpha^* = \overline{S}_\alpha^T)$.

II. Truncated singular value estimation

Instead of trying to reduce the number of unknowns, the $\alpha \leq N_x$ harmonics corresponding to the rectangular sensitivity matrix S_α used in Eq. (10), it is possible to keep the total number of harmonics to be estimated equal to N_x using regularization by truncated singular value decomposition (TSVD) [4]. This regularization technique is based on the square matrix S whose singular value decomposition (SVD) is

$$S = UWV^T \qquad \text{with} \qquad U^*U = UU^* = V^*V = V^*V = I_{N_x},$$

$$\text{with} \qquad W = \text{diag}(w_1, w_2, \cdots, w_{N_x}),$$

$$\text{where} \qquad w_1 \geq w_2 \geq \cdots w_{Nx-1} \geq w_{Nx} \geq 0,$$

$$U = \begin{bmatrix} U_1 & U_2 & \cdots & U_{Nx} \end{bmatrix}; \qquad V = \begin{bmatrix} V_1 & V_2 & \cdots & V_{Nx} \end{bmatrix}$$

(11)

and where w_k, U_k and V_k are the k-th singular value, the k-th left singular vector and the k-th right singular vector respectively. The ordinary least estimator (8) can also be written as

$$\widehat{\widehat{\theta}}_{OLS}^{\,square} = \arg(\min(J(\widetilde{\theta}))) = VW^{-1}U^*\theta^{\,noised}.$$

(12)

The truncated version of this estimator is

$$\widehat{\widehat{\theta}}_\alpha^{\,TSVD} = VW_\alpha^{-1}U^*\theta^{\,noised} \qquad \text{with} \qquad W_\alpha^{-1} = \text{diag}(w_1^{-1}, w_2^{-1}, \cdots, w_\alpha^{-1} \; 0 \; \cdots \; 0 \;).$$

(13)

This estimator is intended to keep the number of estimated N_x unchanged, while using a number of internal degrees of freedom α (the number of the inverse singular values w_k^{-1} different from zero in (13)), which becomes smaller than N_x with a decrease of the dispersion of the estimates since

$$\text{Trace}\left(\text{cov}\left(\widehat{\widehat{\theta}}_\alpha^{\,TSVD}\right)\right) = \sum_{n=1}^{N_x} \text{var}\left(\widehat{\widehat{\theta}}_{n,\,\alpha}^{\,TSVD}\right) = \sigma^2 \sum_{k=1}^{N_x} \frac{1}{w_k^2} \leq \text{Trace}\left(\text{cov}\left(\widehat{\widehat{\theta}}_{OLS}^{\,square}\right)\right),$$

(14)

where cov ( ) is the variance-covariance matrix of a column vector.

The singular values of the sensitivity matrix S calculated over the $]-\ell; \ell]$ interval with the eigenvalues calculated on the larger interval $\alpha_n = n\pi/2\ell$ ($k_v = 2$) are plotted in Fig. 6, together with the eigenvalues $\alpha_n = n\pi/\ell$ ($k_v = 1$).

It is very clear that the inverse problem met here is severely ill-posed since the condition number of matrix S is $\text{cond}(S) = w_1/w_{N_x=200} = 153.9/3.57 \; 10^{-15} = 4.3 \; 10^{16} \approx \infty$. This matrix is clearly singular and regularization is compulsory. If the TSVD is used, it is obvious that the optimum value for the truncation parameter α will be in the region between $90 < \alpha < 110$ where the singular values show a sharp change of level.

Comparison of the variations of the root mean square residual r_{rms} (Eq. (15)) with the α regularization hyperparameter for the rectangular and the TSVD estimation is shown in Fig. 7, where the vertical scale is logarithmic. Rectangular ordinary least square estimation cannot follow the simulated measurements for $\alpha > 20$ where strong oscillations with α appear. The residuals of TSVD estimation meet the level of the standard deviation of the noise, for α between 80 and 90.

$$r_{\text{rms}}\left(\widehat{\theta}_\alpha^{\,reg}\right) = \frac{1}{\sqrt{N_x}} \left\| \theta^{\,noised} - \widehat{\theta}_\alpha^{\,reg} \right\| = \frac{1}{\sqrt{N_x}} \left\| \theta^{\,noised} - S\widehat{\widehat{\theta}}_\alpha^{\,reg} \right\|$$

(15)

with $reg = rect$ or $TSVD$.
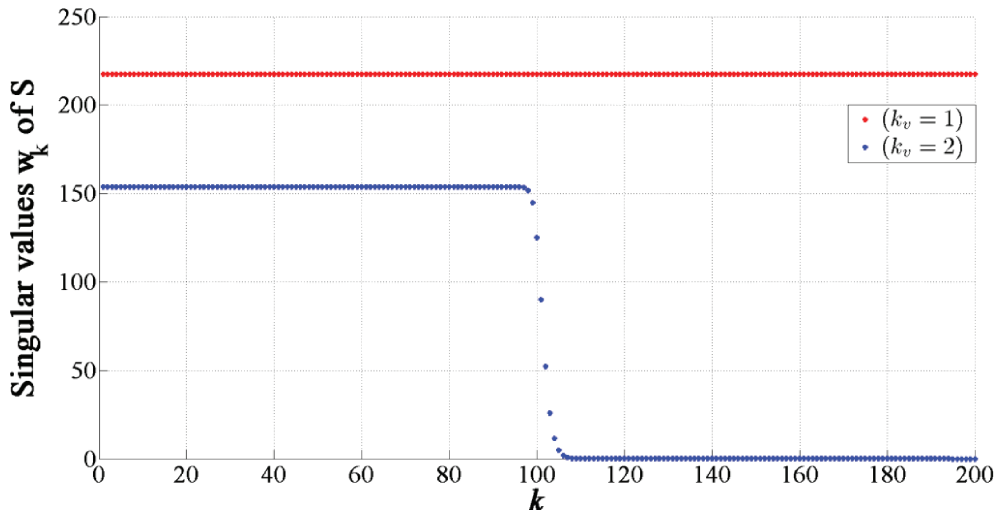
Fig. 6. Singular values of the square sensitivity matrix S for ($k_v = 1$ and 2).
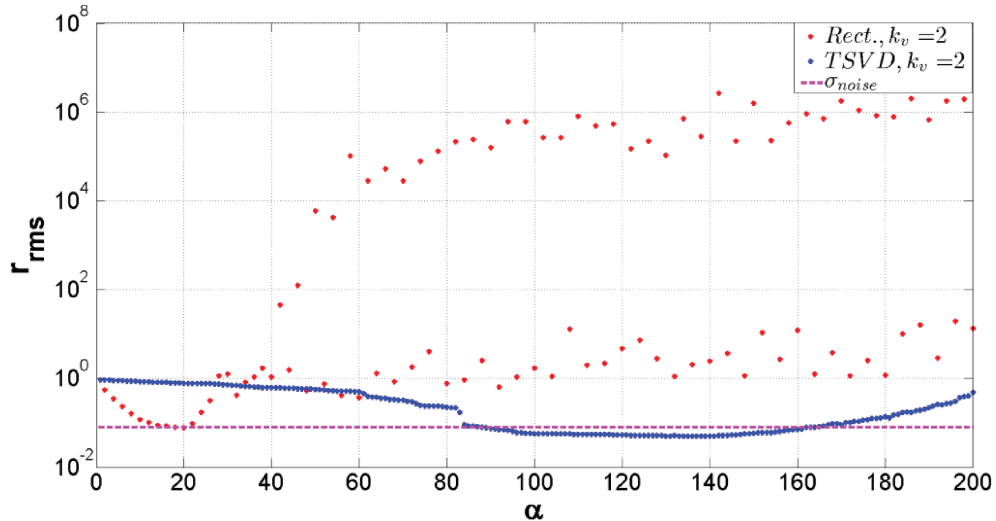
Fig. 7. Root mean square residuals for rectangular and TSVD estimations ($k_v = 2$).

The root mean squares of the errors of the estimates e_{rms} (Eq. (16)) are plotted as a function of α for the rectangular estimation and for the TSVD estimation in Fig. 8, where the vertical scale is logarithmic. For values of α lower than 120, the error is lower for the TSVD estimate, with a minimum being slightly lower than $\alpha = 100$. This corresponds roughly to the value where the r_{rms} is slightly above the noise level (flat region between 80 and 90) in Fig. 7, which corresponds to the discrepancy principle [7]

$$e_{\mathrm{rms}}(\alpha) = \frac{1}{\sqrt{N_x}} \left\| \widehat{\widetilde{\theta}}_\alpha^{\,reg} - \widetilde{\theta}_\alpha^{\,exact} \right\|. \tag{16}$$

The recalculated signal $\boldsymbol{\theta}^{\,recalc} = \boldsymbol{S}\widehat{\widetilde{\boldsymbol{\theta}}}_\alpha^{\,TSVD}$ is plotted together with the exact signal $\boldsymbol{\theta}^{\,exact}$ and with the noised signal $\boldsymbol{\theta}^{\,noised}$ in Fig. 9 for $\alpha = 89$, the fit is good.

The corresponding spectral energy density is presented in Fig. 10. It shows that the estimation on a smaller x interval instead of being on the whole interval of width $2L$, even if it is not perfect is possible using a TSVD regularization.
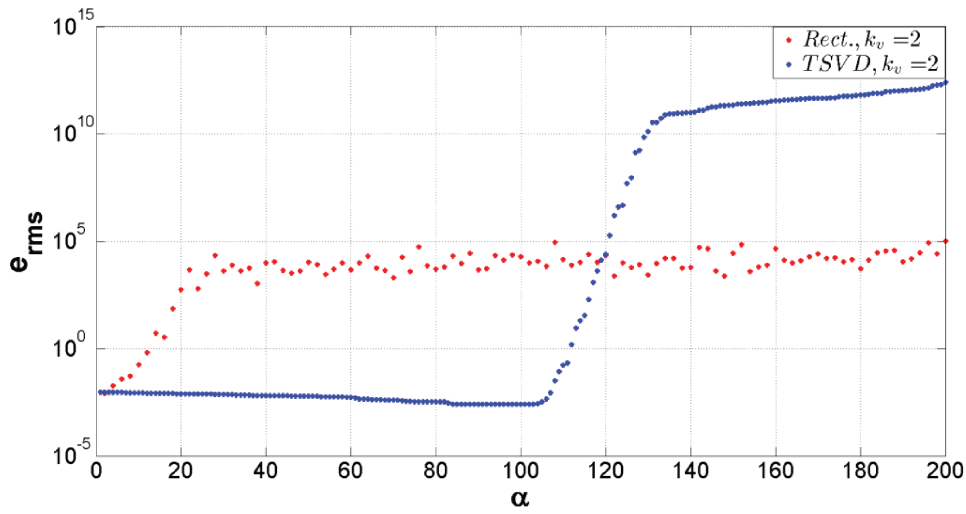
Fig. 8. Root mean square errors of the estimates of the harmonics for rectangular and TSVD estimations $(k_v = 2)$.
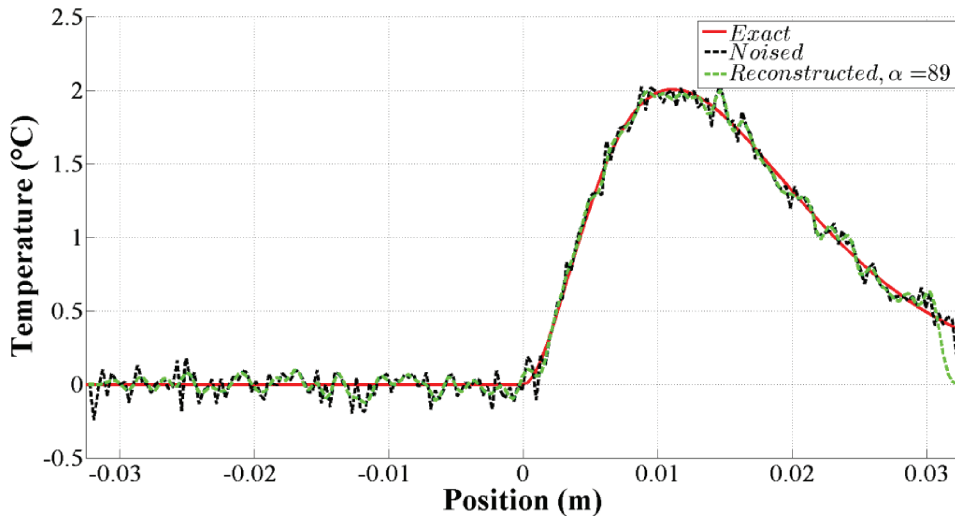
Fig. 9. Exact, noised and reconstructed temperature profiles using TSVD $(k_v = 2)$.
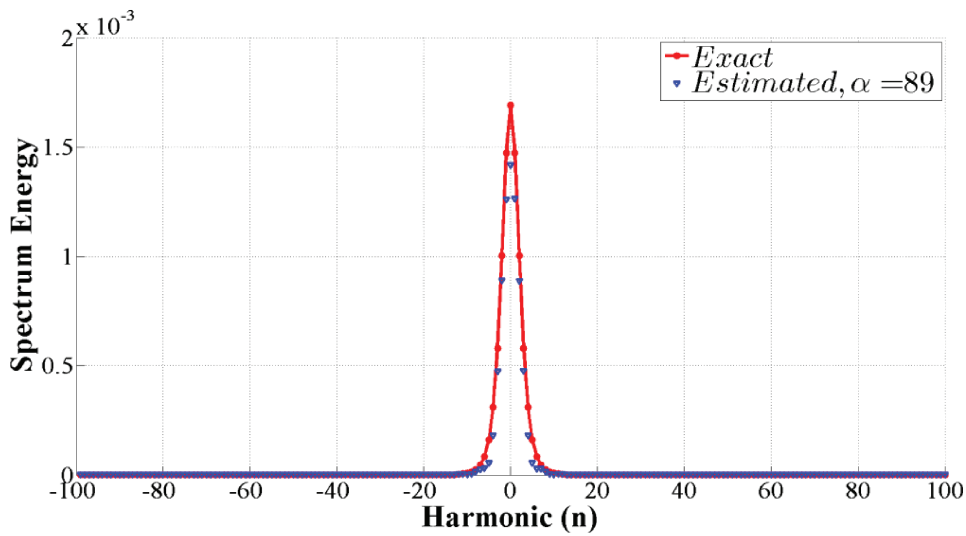
Fig. 10. Spectral energy densities of temperature profiles: exact $(\widetilde{\theta}_n^* \widetilde{\theta}_n)$ and estimated $(\widehat{\widetilde{\theta}}_\alpha^{*TSVD} \widehat{\widetilde{\theta}}_\alpha^{TSVD})$.

From the spectrum estimated previously we can reconstruct the $\boldsymbol{\theta}$ profile not only over the $]-\ell;\ell]$ interval (the distance between the two dotted lines, see Fig. 11) but also outside this interval. We can see that the profile on the interval $]-\ell;\ell]$ is fairly reconstructed but that is not the case outside of this interval.
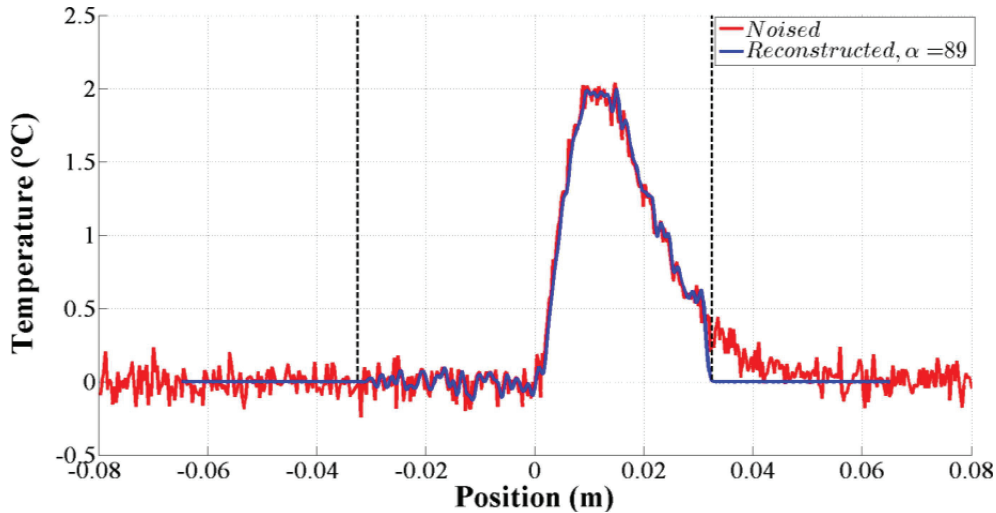
Fig. 11. Noised and reconstructed temperature profiles using TSVD ($k_v = 2$).

The choice of k_v constitutes a delicate point: it should be not too large because in this case α will be small (with a loss in the number of the degrees of freedom), but not too small in order to satisfy the discrepancy principle. Figures 12 and 13 show the root mean square error for the estimated spectrum (with respect to the reference case $L = L_0$) and the root mean square residual that are plotted against the value of the regularization parameter α corresponding to different values of k_v (that is, corresponding to different values of L for the preceding fixed value of ℓ).

This shows quite clearly that there is a relationship between the optimum value of α (regularization parameter) and the virtual length ratio.

Table 1 was constructed, starting from Figs. 12 and 13, to clarify the optimal choices of both k_v and α. In practice, the line giving e_{rms} is not available for a real problem and is only present to test the optimality condition of the discrepancy principle. Let us remark here that our approach is
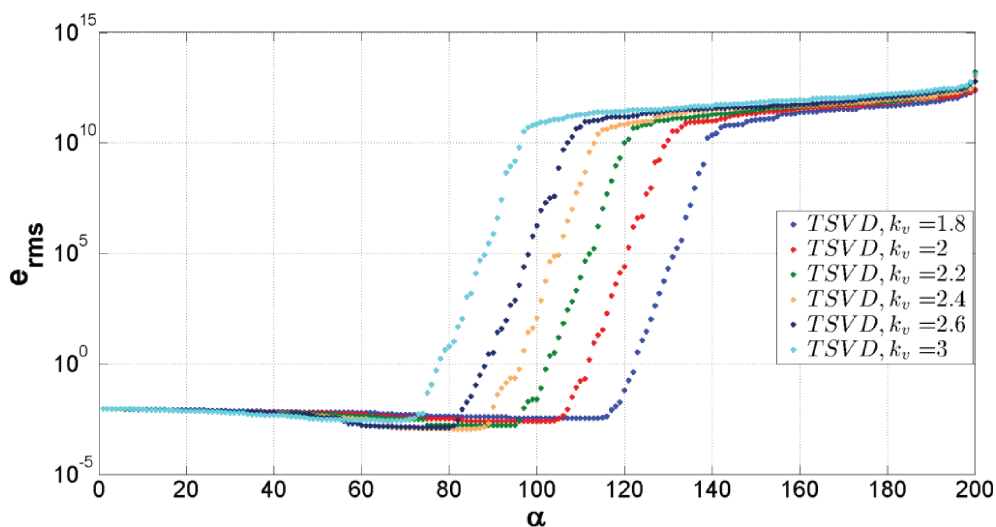
Fig. 12. Root mean square errors of the estimates of the harmonics for TSVD estimation at different k_v.
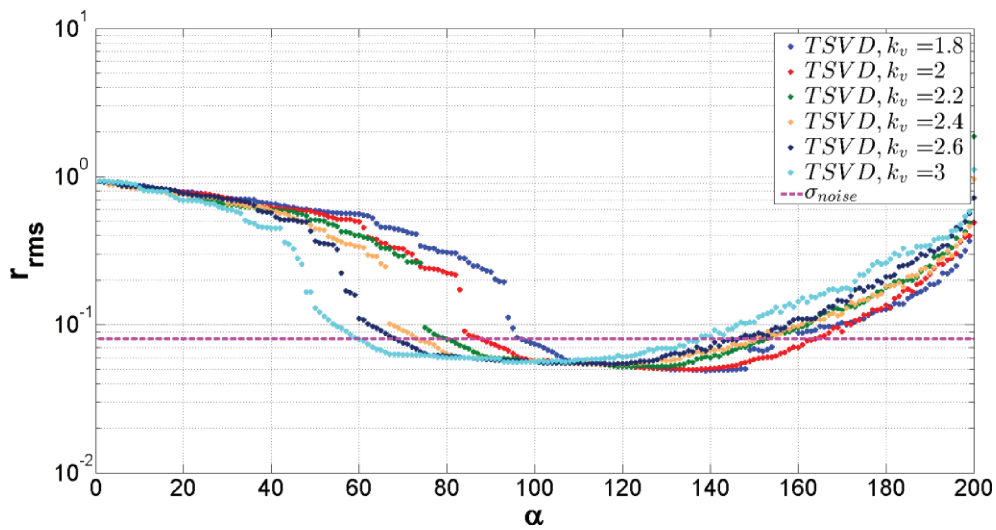
Fig. 13. Root mean square residuals for TSVD estimation at different k_v.

Table 1. Optimization of α for different virtual length ratios k_v.

$k_v = L/\ell$	1	1.8	2	2.2	2.4	2.6	3
α_{opt} based on discrepancy principle using residuals r_{rms}	200 ($\alpha_{opt} = N_x$, no regularization)	96	87	79	73	68	59
α_{opt} based on the lower norm of the e_{rms} error and corresponding lower value of $e_{\mathrm{rms}} \times 10^3$	200 (7.75)	96 (3.54)	89 (2.54)	91 (1.66)	84 (1.11)	77 (1.30)	67 (2.80)
α_{opt} based on Eq. (17)	200	111	100	91	83	77	67

limited to functions $\theta(x)$ that are quite smooth over the $]-\ell; \ell]$, that is, without an abrupt change and with a return to zero on the lower and upper bounds of the $]-L_0; L_0]$ interval in order to get a Fourier reconstruction without discontinuity in $\pm L_0$ (periodicity conditions).

We see that the real optimum (lower value of e_{rms}) is close to the optimum corresponding to the discrepancy principle. The higher the value of k_v chosen, the smaller the optimum value α_{opt} of the TSVD hyperparameter becomes. So, as a rule of thumb, one can adopt the following criterion:

$$\alpha_{opt} \approx N_x/k_v. \tag{17}$$

The corresponding value of α_{opt} is given in the last line of Table 1, it fits quite well the real optimum here.

Concomitantly, the higher the value of k_v, the lower the e_{rms} error till its exact minimum value for $k_v = 2.4$, which is very close to $k_{v0} = L_0/\ell = 2.46$, with an increase of past this value, which is quite normal. So, if a too large value for k_v is chosen, the quality of the estimation of the spectrum will degrade. In practice, it is recommended to make a numerical simulation with k_v as close as possible to the reality.

We have also considered the case $k_v = 1$ in Table 1, which does not require regularization and allows a good fit of the data, see Fig. 4, but with a poor estimation of its spectrum, see Fig. 5 (high value of e_{rms}).

3. Conclusions

We have shown in this paper that estimation of the Fourier spectrum of a temperature profile was possible using measurements over an interval smaller than the space interval where its Fourier transforms are defined. This allowed to take into account ill-defined lateral boundary conditions in problems involving inversion of a temperature profile measured by infrared thermography. These problems are met, for example, in thermal characterization of heat transfer in a flat mini-channel with outside temperature measurements, where the model can be written analytically in a simple way using Fourier transforms of temperature and flux (thermal quadrupoles method).

Let us note that in terms of inversion, this problem is related to data completion [8]. However, here one does not try to extrapolate available data but rather to reconstruct an optimum linear parameterization of a sampled function, where its coefficients, the different Fourier harmonics, have a physical meaning, for example, in heat transfer.

References

[1] Y. Souhar, B. Rémy, A. Degiovanni. Thermal characterization of anisotropic materials at high temperature through integral methods and localized pulsed technique. *International Journal of Thermophysics*, **34**: 322–340, 2013.

[2] Y. Rouizi, D. Maillet, Y. Jannot. Fluid temperature distribution inside a flat mini-channel: semi-analytical wall transfer functions and estimation from temperatures of external faces. *International Journal of Heat and Mass Transfer*, **64**: 331–342, 2013.

[3] Y. Rouizi, W. Al Hadad, D. Maillet, Y. Jannot. Experimental assessment of the fluid bulk temperature profile in a mini-channel through inversion of external surface temperature measurements. *International Journal of Heat and Mass Transfer*, **83**: 522–535, 2015.

[4] W. Al Hadad, Y. Rouizi, Y. Jannot, B. Rémy, D. Maillet. Estimation of the heat transferred to a fluid minichannel by an inverse technique. *Proceedings of the 15th International Heat Transfer Conference, IHTC-15*, Kyoto, Begell House, August, 2014. doi: 10.1615/IHTC15.inv.009190

[5] D. Maillet, S. André, J.C. Batsale, A. Degiovanni, C. Moyne. *Thermal quadrupoles – solving the heat equation through integral transforms*. Wiley, Chichester, England, 2000.

[6] A. Bendada, F. Erchiqui, M. Lamontagne. Pulsed thermography in the evaluation of an aircraft composite using 3D thermal quadrupoles and mathematical perturbations. *Inverse Problems*, **21**: 857–877, 2005.

[7] R.C. Aster, B. Borchers, C.H. Thurber. *Parameter Estimation and Inverse Problems*, Second edition, Elsevier Edition, Academic Press, Amsterdam, The Netherlands, 2012.

[8] Y. Boukari, H. Haddar. A convergent data completion algorithm using surface integral equations. *Inverse Problems, Institute of Physics: Hybrid Open Access*, 21 pages, 2015.